Journal of Cerebral Blood Flow & Metabolism (2014) 34, 1197–1204

www.jcbfm.com

ORIGINAL ARTICLE

The size of blood–brain barrier opening induced by focused ultrasound is dictated by the acoustic pressure

Hong Chen[1] and Elisa E Konofagou[1,2]

Focused ultrasound (FUS) in combination with microbubbles (MBs) has been successfully used in the delivery of various-size therapeutic agents across the blood–brain barrier (BBB). This study revealed that FUS-induced BBB opening size, defined by the size of the largest molecule that can permeate through the BBB, can be controlled by the acoustic pressure as dictated by cavitational mechanisms. Focused ultrasound was applied onto the mouse hippocampus in the presence of systemically administered MBs for trans-BBB delivery of fluorescently labeled dextrans with molecular weights 3 to 2,000 kDa (hydrodynamic diameter: 2.3 to 54.4 nm). The dextran delivery outcomes were evaluated using *ex vivo* fluorescence imaging. Cavitation detection was employed to monitor the MB cavitation activity associated with the delivery of these agents. It was found that the BBB opening size was smaller than 3 kDa (2.3 nm) at 0.31 MPa, up to 70 kDa (10.2 nm) at 0.51 MPa, and up to 2,000 kDa (54.4 nm) at 0.84 MPa. Relatively smaller opening size (up to 70 kDa) was achieved with stable cavitation only; however, inertial cavitation was associated with relatively larger BBB opening size (above 500 kDa). These findings indicate that the BBB opening size can be controlled by the acoustic pressure and predicted using cavitation detection.

Journal of Cerebral Blood Flow & Metabolism (2014) **34,** 1197–1204; doi:10.1038/jcbfm.2014.71; published online 30 April 2014

Keywords: blood–brain barrier; different-size agents; drug delivery; microbubbles; ultrasound

INTRODUCTION

Brain diseases or disorders can be difficult to treat through systemic delivery of therapeutic agents, because most agents are blocked by a natural barrier in the brain: the blood–brain barrier (BBB). This barrier is a specialized structure existing between the cerebral vasculature and the brain parenchyma. Different from barriers between peripheral vasculature and other organs in the body, both the transcellular and paracellular pathways are strictly restricted by the BBB because of the paucity of pinocytotic vesicles in cerebral vessels and the presence of tight junctions between adjacent endothelial cells. Certain small lipid-soluble drugs with a molecular weight (MW) <400 Da may cross the BBB.[1] Unfortunately, the majority of the therapeutic agents are larger than the size limit, and thus cannot cross the BBB. Focused ultrasound (FUS) in combination with microbubbles (MBs) is an emerging technique that has been successfully used in trans-BBB delivery of therapeutic agents of various sizes, such as chemotherapeutic drugs (MW $\sim$500 Da),[2] neurotrophins (MW $\sim$20 kDa),[3] antibodies (MW $\sim$150 kDa),[4] and gene vectors (MW $\sim$4 MDa).[5]

Although neurosurgical, pharmacologic, or physiologic strategies have been developed to circumvent the BBB for brain drug delivery,[1] transcranial FUS in combination with MBs is the only known technique that can induce localized and reversible BBB opening.[6,7] Externally generated ultrasound waves can be focused through the intact scalp and skull onto a small focal region (on the order of millimeters) deep into the subcortical structures, which allows highly precise and noninvasive targeting of brain tissues. Microbubbles, which are gas-filled bubbles coated by protein or lipid shells (diameters of 1 to 10 μm), were originally introduced into the clinic as blood-pool ultrasound contrast agents, circulating in the vascular space. When encountering an ultrasound beam, they cavitate, which is a broad term for various ultrasound-induced bubble activities, including their volumetric oscillation and collapse. It has been found that MB cavitation in the cerebral vasculature can induce localized BBB opening by stretching the tight junctions and stimulating the formation of vesicles, enabling paracellular and transcellular transports, respectively.[7,8] Paracellular transport through intercellular tight junctions is size selective in that only molecules smaller than the gaps between tight junctions can go through; in contrast, transcytotic transport by cellular vesicles carrying the molecules through the endothelial cells is size-independent as vesicles are much larger than most therapeutic agents.[9,10]

Extensive research has been performed to show the great potential of FUS in the delivery of various-size therapeutic agents; however, studies are limited on the FUS-induced BBB opening size, defined by the size of the largest molecule that can permeate through the BBB. Almost all previous studies used only one specific-size agent and found the treatment parameters that contributed to the successful delivery of that agent. Only two reported studies have compared the delivery outcomes of different-size agents to assess the maximum BBB opening size. In the first study, Choi *et al*[11] used fluorescently labeled dextrans of 3, 70, and 2,000 kDa with respective hydrodynamic diameters of about 2.3, 10.2, and 54.4 nm as model drugs. They found that using 1.525 MHz FUS at 0.57 MPa, 3 and 70 kDa dextrans were delivered trans-BBB, while 2,000 kDa dextran was not, which suggested that there was a size limit associated with FUS-induced BBB opening. In the second study, Marty *et al*[12] used magnetic resonance contrast

[1]Department of Biomedical Engineering, Columbia University, New York, New York, USA and [2]Department of Radiology, Columbia University, New York, New York, USA. Correspondence: Dr EE Konofagou, Department of Biomedical Engineering, Columbia University, 351 Engineering Terrace, Mail Code 8904, 1210 Amsterdam Avenue, New York, NY, USA.
E-mail: ek2191@columbia.edu
This study was supported by NIH grants R01 EB009041 and R01 AG038961 and the Kinetics foundation.
Received 20 December 2013; revised 16 March 2014; accepted 21 March 2014; published online 30 April 2014

agents of different hydrodynamic diameter (1 to 65 nm) as model drugs and found that the maximum BBB opening size varied between 25 and 65 nm using 1.5 MHz FUS at 0.45 MPa. However, as only a single set of fixed ultrasound parameters was used, the dependence of the BBB opening size on acoustic parameters remained unexplored.

Depending on the acoustic pressure, MB cavitation can range from stable cavitation (SC) to inertial cavitation (IC), which are considered to be the main physical mechanisms responsible for FUS-induced BBB opening.[13] At low pressure, MBs undergo stable volumetric oscillation, or SC. The oscillating MBs can induce 'pushing' and 'pulling' forces, as well as shear forces, on the endothelium, which likely increase vascular permeability[14] without causing any vascular damage.[15] At high pressure, larger MB expansion could induce IC, leading to sudden collapse of the MBs. Microbubbles exert forces on the vessels to a much larger extend and can generate liquid microjets.[16] This IC behavior is more forceful and may increase BBB permeability to a larger extent. IC has been shown to be associated with microdamage to the cerebral vessels.[15,17] Under the acoustic parameters reported for BBB opening so far, the most dominant damaging effect induced by IC is minor extravasation of blood components such as red blood cells at the sonicated locations.[17–21] No ischemic or apoptotic regions were detected that would indicate a compromised blood supply.[21] Recent work in nonhuman primates showed that the minimal tissue damage induced after repeated BBB disruption did not cause any detectable behavioral effects.[20] The acoustic emissions from SC and IC have been detected by passive cavitation detection (PCD) to monitor MB behavior and improve the safety of BBB opening.[17,18,20,22] Until now, PCD has only been used in cavitation detection during FUS-enhanced delivery of magnetic resonance imaging contrast agents (MW $<$ 1 kDa)[17,18,20,22] and 3 kDa dextran.[23] No cavitation detection has been performed to monitor FUS-activated MB behaviors in the delivery of any other larger agents; consequently, the physical mechanisms for how FUS in combination with MBs deliver different-size agents across the BBB have not been fully understood.

The main purpose of the present study was thus threefold: (1) to assess the dependence of the BBB opening size on acoustic parameters, specifically the acoustic pressure; (2) to identify MB cavitation behaviors associated with the trans-BBB delivery of different-size agents; (3) to evaluate the histologic effects associated with the delivery of different-size agents. The BBB opening size was assessed using fluorescently labeled dextrans of 3 to 2,000 kDa. Delivery outcomes of these intravenously administered dextrans after FUS sonication were evaluated based on fluorescence images of brain slices. Passive cavitation detection was performed to monitor MB cavitation behaviors during sonication. Histologic analysis was performed for safety evaluation. For the first time, we found the BBB opening size was controllable by the acoustic pressure, and revealed the physical mechanisms associated with the trans-BBB delivery of different-size agents. The knowledge gained from this study is important toward a better understanding of the mechanisms for FUS-induced BBB opening and provides guidance for developing agent size-specific FUS treatment protocols.

MATERIALS AND METHODS

Preparation of Animals

In accordance with the National Institutes of Health Guidelines for animal research, all animal procedures for these experiments were reviewed and approved by the Institutional Animal Care and Use Committee of the Columbia University. This study used four different-size fluorescein-labeled dextrans (3, 70, 500, and 2,000 kDa) to assess their delivery outcomes under three acoustic pressure levels (0.31, 0.51, and 0.84 MPa). Therefore, there were 12 study groups (effective sample size: 4 mice per group) (Table 1). Wild-type adult male mice (strain: C57BL/6, age: 6 to 8 weeks, masses: 22.5 ± 1.6 g (mean ± standard deviation); Harlan Sprague Dawley, Indianapolis, IN, USA) were used. During the whole procedure, the mice were anesthetized with isoflurane in oxygen. They were placed prone on a heating pad with a constant temperature output of ~40°C to maintain their body temperature. Their heads were immobilized by a stereotaxic frame (David Kopf Instruments, Tujunga, CA, USA). Their head positions were adjusted so that the skin surface at the locations of the bregma and the lambda was evenly leveled by visual inspection, so that the sutures on the heads could later be reliably used for FUS targeting of a brain region. The fur on the head was removed with an electrical trimmer and a depilatory cream. The scalp and skull remained intact.

Focused Ultrasound Experimental Setup

A schematic illustration of the main components of the system is shown in Figure 1A. A single-element FUS transducer (center frequency: 1.5 MHz, focal depth: 60 mm, diameter: 60 mm; Imasonic, Besancon, France) was driven by a function generator (33220A; Agilent, Palo Alto, CA, USA) through a nominal 50 dB gain power amplifier (325LA; E&I, Rochester, NY, USA). The transducer was attached to a three-dimensional positioning system (Velmex, Lachine, QC, Canada). A custom-built truncated cone was attached to the transducer and filled with degassed water to provide acoustic coupling. The cone was immersed in a degassed-water container. The bottom of the water container had a window sealed with an almost acoustically and optically transparent membrane. The container was placed on the mouse head and coupled with degassed ultrasound gel.

Acoustic emissions arising from MB cavitation were acquired by a passive cavitation detector (center frequency 10 MHz; focal length 60 mm; Olympus NDT, Waltham, MA, USA). It was positioned through a central hole of the FUS transducer and confocally aligned with the FUS transducer. The signals received by the detector were amplified by 20 dB (Model 5800; Panametrics-NDT, Waltham, MA, USA) and then digitized (Razor Express CompuScope 1422; Gage Applied Technologies, Inc., Lachine, QC, Canada) at a sampling frequency of 50 MHz. A custom Matlab program (Mathworks Inc., Sherborn, MA, USA) was used to acquire the acoustic emission signals during the exposure of each ultrasound pulse.

The FUS transducer was characterized as described elsewhere.[24] The pressures reported here were all peak-negative pressures derated by 18% of that measured in water to account for skull attenuation.[24] The dimensions of the beam in water had a lateral and axial full-width at half-maximum pressure of 1.3 and 13.0 mm, respectively.

Focused Ultrasound Sonication

Commercially available Definity MBs (mean diameter range: 1.1 to 3.3 μm, Lantheus Medical Imaging, North Billerica, MA, USA) were used in this study. Those are octafluoropropane gas bubbles coated by a lipid shell. After activation following the manufacturer's instructions, MBs were injected into each mouse through the tail vein at a dose of 0.05 μL/g of body weight. This dose was comparable to the clinical dose (0.01 μL/g) allowed by the FDA (Food and Drug Administration) for diagnostic purposes in humans.

Fluorescein-tagged dextrans (Invitrogen, Carlsbad, CA, USA) of four sets of distinct MWs were used as model drugs: 3 kDa (D3306, hydrodynamic diameter D_H ~2.3 nm), 70 kDa (D1822, D_H ~10.2 nm), 500 kDa (D7136, D_H ~30.6 nm), and 2,000 kDa (D7137, D_H ~54.4 nm).[11,25] For each study, 2 mg of one specific-MW dextran was dissolved in 100 μL saline and injected to one mouse. Dextrans were chosen as model therapeutic compounds because they are known to be biologically and chemically inert and available in various MWs. These four dextrans were used to represent the broad MW range of the therapeutic agents that have been successfully delivered across the BBB. Fluorescein-labeled dextrans were selected because they have the widest range of MWs among all the commercially available fluorescently labeled dextrans.

The left hippocampus of each mouse was selected as the targeted region of interest and the right hippocampus was used as a control. Each animal served as its own control, thereby reducing the variability caused by physiologic differences among animals. Before sonication, a grid system to locate the sutures of the skull was used for the targeting procedure (see ref. 24 for more details). Briefly, to target the left hippocampus, the FUS transducer was laterally moved 3 mm to the left of the sagittal suture and 2 mm anterior of the lambdoid suture. The focal point of the FUS was placed 3 mm beneath the skull, which was at about the center of the hippocampus.

Ultrasound sonication with a pulse rate of 5 Hz and a pulse duration of 1.3 ms (2,000 cycles) was applied to the left hippocampus with a peak-negative pressure of 0.31, 0.51, or 0.84 MPa. About 6 seconds after sonication started, MBs mixed with one of the four dextrans were injected

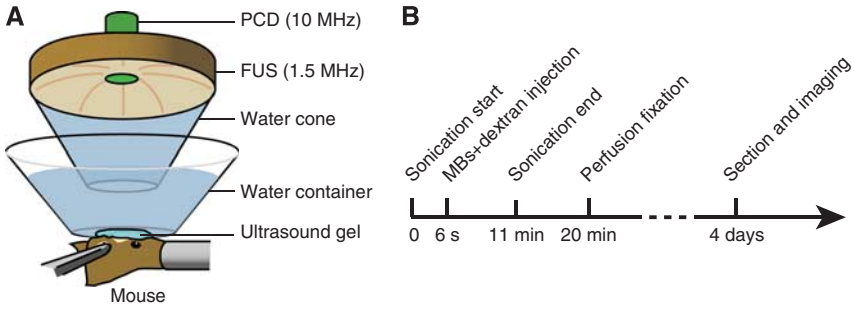

Figure 1. (**A**) Schematic illustration of the experimental setup. A 1.5-MHz single element focused ultrasound (FUS) transducer was used for blood–brain barrier opening. It was confocally aligned with a transducer for passive cavitation detection (PCD). The left hippocampus of each mouse was targeted during sonication and the right hippocampus was used as the control. (**B**) Illustration of the experimental timeline. Sonication started ~6 seconds before the injection of a mixture of Definity microbubbles and one dextran with a molecular weight of 3, 70, 500 or 2,000 kDa. During the 11-minute sonication, cavitation detection was performed. The mice were transcardially perfused and fixed at ~20 minutes after dextran injection and then the brain tissue was sectioned for fluorescence imaging.

into the tail vein of each mouse (see the experiment timeline in Figure 1B). The cavitation emission signals acquired within that 6 seconds provided baselines for cavitation quantification. The total sonication time was 11 minutes.

Blood–Brain Barrier Opening Quantification

At 20-minute after the dextran injection (Figure 1B), the mice were transcardially perfused with 30 mL of phosphate-buffered saline and 60 mL of 4% paraformaldehyde. The brains were extracted from the skull on the next day and postfixed in paraformaldehyde overnight, followed by cryoprotection for another 24 hours. The brains were then sequentially sectioned using a cryostat into 60-μm-thick slides in the horizontal orientation. Sections were imaged using a microscope (BX61; Olympus, Melville, NY, USA) equipped with a fluorescein filter set (excitation filter: 467 to 498 nm; emission filter: 513 to 556 nm) and an Olympus DP30BW digital camera. Five sequential sections with two dorsal sections, two ventral sections, and a reference midline section, which were determined by anatomical landmarks, were selected for analysis using a custom Matlab (Mathworks Inc., Natick, MA, USA) program as follows.

The left (sonicated) and right (nonsonicated) hippocampi on each section were manually outlined. A circle with a diameter of 200 pixels was selected outside the hippocampi, and three times of the standard deviation above the mean pixel intensity within the circle was used to represent the background autofluorescence intensity. To compare among animals, all the fluorescence images were normalized by dividing their corresponding background fluorescence intensities. Fluorescence pixels due to dextran delivery were separated from background autofluorescence by identifying pixels with intensities above the background autofluorescence intensity in both hippocampi. On each section, we then calculated the fluorescence enhancement by subtracting the total intensities of the identified pixels on the left from that on the right. We also calculated the percent of fluorescently enhanced pixel numbers by subtracting the total number of identified pixels on the right from that on the left and then dividing the total number of pixels in the left hippocampus. Finally, two parameters were used to quantify the trans-BBB delivery outcomes for each brain. (1) Average fluorescence intensity was defined to represent the relative amounts of dextrans delivered to the targeted hippocampus. It was calculated by the mean of the fluorescence enhancement across the five sequential sections. (2) Average area of fluorescence was defined to estimate the spatial distributions of the delivered dextrans, which represented how diffuse the dextrans were. It was calculated by the mean of the percent fluorescently enhanced pixel numbers for the five selected sections. Special care was taken so that brains with perfusion or sectioning artifacts were not included for the analysis.

Microbubble Cavitation Emission Quantification

The acoustic emissions from the ultrasound-activated MBs were detected and quantified using stable cavitation dose (SCD) and inertial cavitation dose (ICD) to assess the 'amount' of energy associated with the two types of cavitation activities: SC and IC, respectively. They were calculated on the basis of the frequency content of the acoustic emission: SCD was derived from the harmonic emissions while ICD was from the broadband emissions.[23,26] Mice with abnormal cavitation signals were not included (for example, cases showing high superharmonics before the injection of MBs, caused by air bubbles trapped on the skin or in the ultrasound gel).

A fast Fourier transform was performed for each signal acquired during the sonication of each ultrasound pulse. Frequency spectra between the 4th and 10th harmonics were used for SC and IC quantification to eliminate any contributions from the FUS beam. The harmonic (nf, $n=4$, 5, ..., 10) and ultraharmonic (nf/2, $n=9$, 11, … 21) frequencies were filtered out by excluding $\pm$150 kHz bandwidths around each of them.[18] This bandwidth was designed to be filtered to ensure that SC response was not included in the IC calculation. The root mean square of the filtered spectrum was calculated to represent the IC level for each pulse. Meanwhile, the harmonic levels were obtained by first calculating the root mean square of the maximum amplitudes within the $\pm$150 kHz bandwidths of all harmonics, and then subtracting the corresponding IC level so that the IC activity was not included in the SC quantification. Levels of IC and SC were calculated for all the pulses acquired during the 11-minute sonication.

To minimize variation caused by differences among animals, signals acquired within the initial 6 seconds before the injection of MBs were used to quantify the background cavitation activities. The background SC level was defined by three standard deviations above the mean of the background SC level. Stable cavitation dose was calculated by integrating the SC level above the background through the entire exposure 'on' time ('on' time = pulse length $\times$ total number of pulses). The ICD was similarly calculated using the IC levels of the signals acquired before and after the injection of MBs.

Histologic Analysis

Whole brain histologic examinations were performed using hematoxylin and eosin (H&E) staining for general histology. Following the same treatment protocol described before, six additional mice after sonication at 0.51 MPa ($n=3$) and 0.84 MPa ($n=3$) were perfused and fixed in 4% paraformaldehyde. After postfixation processing, the brains were paraffin embedded and then sectioned horizontally at 6 μm thickness in 10 separate levels with 180 μm intervals. At each level, four sections were acquired and stained with H&E. Bright-field images of the stained sections were acquired using the same microscope (BX61; Olympus) as that used for fluorescence imaging but with an Olympus DP25 camera. Histologic evaluation was performed by a trained observer without knowledge of the location and parameters of sonication. Both the sonicated and non-sonicated hippocampi were evaluated.

Statistical Analysis

Statistical analysis was performed using GraphPad Prism (Version 5.01, La Jolla, CA, USA). For each study group (Table 1), the mean $\pm$ standard deviation of the average fluorescence intensity and area of fluorescence for each group were calculated. Successful dextran delivery was concluded if both the average fluorescence intensity and the area of fluorescence were statistically significantly higher than zero (one-tailed, one-sample Student's *t*-tests). Unpaired two-tailed Student's *t*-tests were used to determine whether the ICD and the SCD were significantly different between any two groups. A P value of <0.05 was considered to represent a significant difference in all the analyses.

RESULTS

Focused Ultrasound-Induced Blood–Brain Barrier Opening

Figure 2 shows representative fluorescence images obtained from mice administered with the four dextrans and sonicated at their left hippocampi at a pressure of 0.84 MPa. Images on the left exhibited the successful delivery of the four dextrans in the FUS-targeted hippocampi; images on the right display the corresponding nonsonicated, contralateral hippocampi. Each pair of images was obtained from a mouse with the highest average fluorescence intensity, as well as the highest percent area of fluorescence, of one specific-size dextran. The control hippocampi showed no or minimal dextran accumulation. In contrast, FUS-treated hippocampi showed enhancement of all the four agents, but with distinct characteristics. A single sonication resulted in an almost homogeneous distribution of 3 kDa dextran throughout the left hippocampus (Figure 2A). When the dextran size increased to 70 kDa (Figure 2C), fluorescence was less homogenously distributed compared with that of the 3-kDa dextran case. The 500-kDa dextran case (Figure 2E) showed significantly lower total fluorescence with less diffusion in the left hippocampus compared with the other two smaller-size dextrans. In the hippocampus injected with 2,000 kDa dextran (Figure 2G), the level of fluorescence was the lowest among the four dextrans and the spatial distribution of fluorescence was characterized by isolated spots. Quantitative assessment indicated that the average fluorescence intensities for the four cases were 1.47×10^6, 0.44×10^6, 0.17×10^6, and 0.07×10^6, respectively; and the average percent areas of fluorescence were 90.11%, 28.20%, 11.27%, and 2.76%, respectively. In summary, it was shown that as the dextran MW increased, not only did the fluorescence intensity decrease but also its distribution became increasingly heterogeneous in the targeted hippocampi.

Figure 3 provides a summary of the quantification results for the delivery outcomes of the four dextrans at different pressures. Detailed statistical information of the BBB opening outcomes is summarized in Table 1. At 0.31 MPa, none of the four tested dextrans was significantly delivered across the BBB after FUS sonication. At 0.51 MPa, only relatively smaller-size dextrans (3 and 70 kDa) were successfully delivered but not the relative larger-size dextrans (500 and 2,000 kDa). All dextrans were delivered across the BBB when the pressure increased to 0.84 MPa. This is indicative that the BBB opening size was smaller than 3 kDa ($D_H \sim 2.3$ nm) at 0.31 MPa, up to 70 kDa ($D_H \sim 10.2$ nm) at 0.51 MPa, and up to 2,000 kDa ($D_H \sim 54.4$ nm) at 0.84 MPa. Figure 3 also shows that as the dextran MW increased, the fluorescence intensity and area of fluorescence decreased at 0.84 MPa, which was consistent with the previous observation based on Figure 2. The mean fluorescence intensity in the case of 3 kDa dextran at 0.84 MPa was 4.21, 11.09, and 24.40 folds of that in the cases of the 70, 500, and 2,000 kDa dextrans, respectively (Table 1). The mean area of fluorescence for the four dextrans (3, 70, 500, and 2,000 kDa) at 0.84 MPa was 82.66%, 25.55%, 8.53%, and 2.23%, respectively (Table 1). It should be pointed out that although larger-size dextrans were successfully delivered across the BBB at 0.84 MPa, the fluorescence intensity and area of fluorescence decreased dramatically as the dextran size increased.

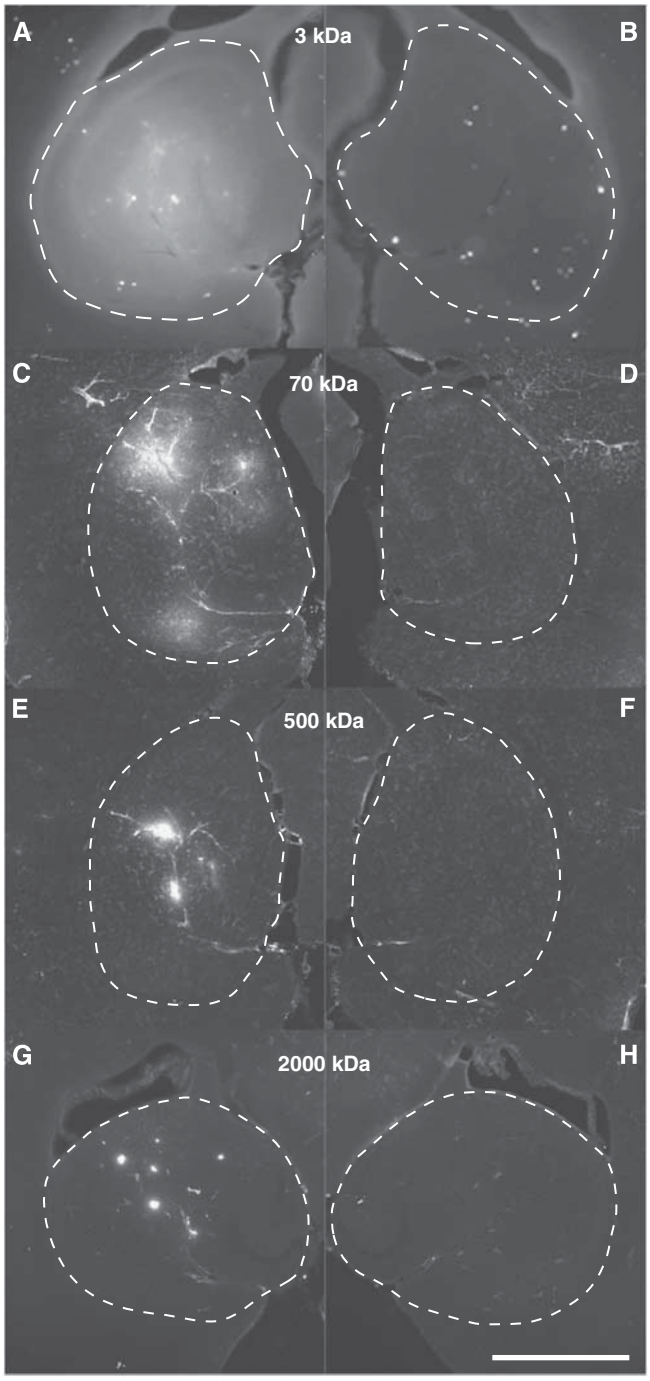

Figure 2. Horizontal sections of the left (sonicated) and right (nonsonicated) hippocampal regions of four mouse brains injected with different-size dextrans: (**A**, **B**) 3 kDa, (**C**, **D**) 70 kDa, (**E**, **F**) 500 kDa, and (**G**, **H**) 2,000 kDa. The dash lines highlight the boundaries of the hippocampal regions. The ultrasound pressure was 0.84 MPa for the four cases. These images show that higher amounts and larger areas of dextran delivery were achieved for smaller-size dextrans. The scale bar represents 1 mm.

Microbubble Cavitation Emissions

Figure 4 summarizes ICDs and SCDs at the three pressure levels for the four different-size dextrans. Microbubble cavitation was independent of the dextran MWs, as no statistically significant difference was found in ICD or SCD among the four dextrans. Therefore, results obtained for different-size dextrans at the same pressure were plotted together. The mean SCD shows a trend of increase with pressure; however, no significant difference among the different groups was found (Figure 4A). The ICD at 0.84 MPa was statistically higher than those at 0.51 and 0.31 MPa (Figure 4B), indicating that the threshold for IC was between 0.51 and 0.84 MPa.

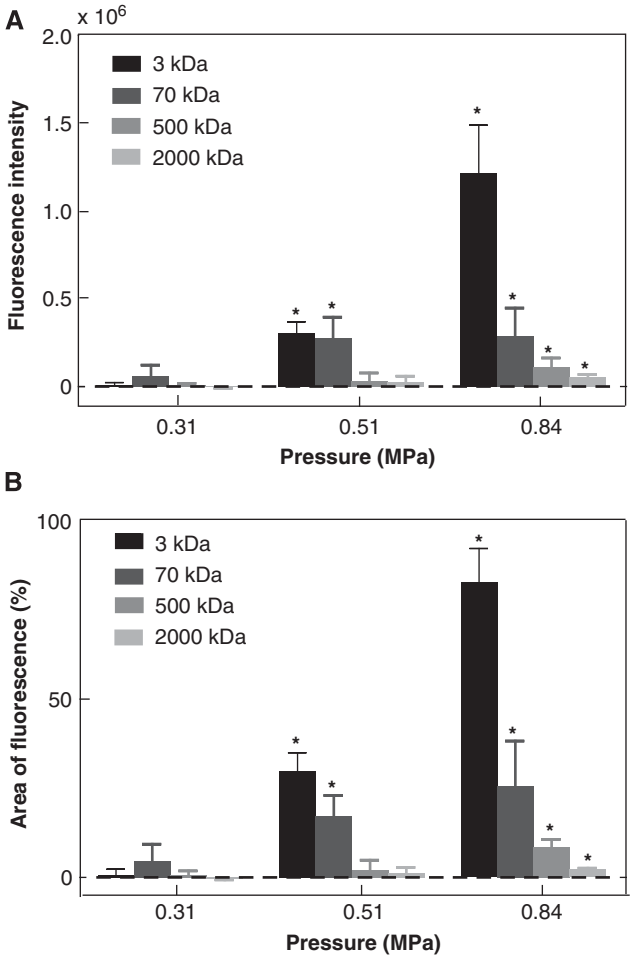

Figure 3. (**A**) Average fluorescence intensity and (**B**) average area of fluorescence for the 3, 70, 500, and 2,000 kDa dextrans sonicated at 0.31, 0.51, and 0.84 MPa. The pressure threshold for significant increases in both fluorescence and area of fluorescence was 0.51 MPa for 3 and 70 kDa dextrans. But it increased to 0.84 MPa for the 500 and 2,000 kDa dextrans. Stars indicate groups with fluorescence intensity or area of fluorescence statistically significant higher than zero ($P < 0.05$).

Histologic Effects

Histologic analysis was performed on additional mouse brains sonicated at 0.51 or 0.84 MPa, which were the pressure thresholds for significant increases in the delivery of relative smaller-size dextrans (3 and 70 kDa) and larger-size dextrans (500 and 2,000 kDa), respectively. At 0.51 MPa, which is below the IC threshold, no tissue damaging effects, such as dead neurons, necrotic sites, or hemorrhage, were detected in the FUS-sonicated hippocampi (Figure 5A), as well as the nonsonicated hippocampi (Figure 5B), in all the three mouse brains. At 0.84 MPa, which is above the IC threshold, two out of the three mouse brains sonicated at 0.84 MPa showed minimal microscopic damage. Microscopic images from the one with more obvious damage are shown in Figures 5C and D. A few extravasated red blood cells and a small area of microvacuolations were found only within the FUS-sonicated hippocampus (Figure 5C), while the nonsonicated hippocampus remained intact (Figure 5D). In summary, no microscopic damage was associated with the delivery of relative smaller-size dextrans (3 and 70 kDa), while minimal microscopic tissue damage could be associated with the delivery of relative larger-size dextrans (500 and 2,000 kDa).

A summary of our findings is as follows. (1) The pressure threshold for a statistically significant increase in the delivery of 3 and 70 kDa dextrans was 0.51 MPa. Meanwhile, a significant increase in ICD was observed only at 0.84 MPa. These results indicated that significant enhancement in the delivery of 3 and 70 kDa dextrans can occur with SC only, without any microscopic tissue damage. (2) The threshold for a significant increase in the delivery of 500 and 2,000 kDa dextrans was 0.84 MPa, which was also the pressure at which significant IC was observed with no difference in SC. This suggested that IC was the main mechanism for the delivery of 500 and 2,000 kDa dextrans. Minimal microscopic damage can be associated with their delivery. These two findings together indicated: (1) trans-BBB delivery of different-size agents through FUS-induced BBB opening depended on the acoustic pressure; and (2) the BBB opening size was dictated by cavitational mechanisms.

DISCUSSION

Despite a rapidly growing number of studies in FUS-induced BBB opening, studies on the BBB opening size are limited. For the first time, we showed that the FUS-induced BBB opening size depended on the acoustic pressure; and revealed that the cavitational mechanisms were different for the significant delivery of different-size agents.

Table 1. Summary of the BBB opening quantification results

Group	*# Of mice*	*Dextran MW (kDa)*	*Pressure (MPa)*	*Fluorescence intensity mean ± s.d. (× 10^6)*	P *value (fluorescence intensity > 0)*	*Area of fluorescence mean ± s.d. (%)*	P *value (area of fluorescence > 0)*	*Successful delivery?*
1	4	3	0.31	0.01 ± 0.02	0.20	0.75 ± 1.53	0.20	No
2	4	70	0.31	0.06 ± 0.06	0.08	4.57 ± 4.75	0.08	No
3	4	500	0.31	0.01 ± 0.01	0.08	0.64 ± 1.17	0.18	No
4	4	2,000	0.31	− 0.01 ± 0.01	0.93	− 0.39 ± 0.31	0.95	No
5	4	3	0.51	0.31 ± 0.06	0.00	29.93 ± 5.00	0.00	Yes
6	4	70	0.51	0.28 ± 0.12	0.01	17.15 ± 5.79	0.01	Yes
7	4	500	0.51	0.03 ± 0.04	0.11	2.17 ± 2.70	0.10	No
8	4	2,000	0.51	0.02 ± 0.03	0.10	1.28 ± 1.51	0.09	No
9	4	3	0.84	1.22 ± 0.27	0.00	82.66 ± 9.55	0.00	Yes
10	4	70	0.84	0.29 ± 0.16	0.02	25.55 ± 12.65	0.01	Yes
11	4	500	0.84	0.11 ± 0.05	0.01	8.53 ± 2.09	0.00	Yes
12	4	2,000	0.84	0.05 ± 0.02	0.01	2.23 ± 0.37	0.00	Yes

BBB, blood–brain barrier; MW, molecular weight.

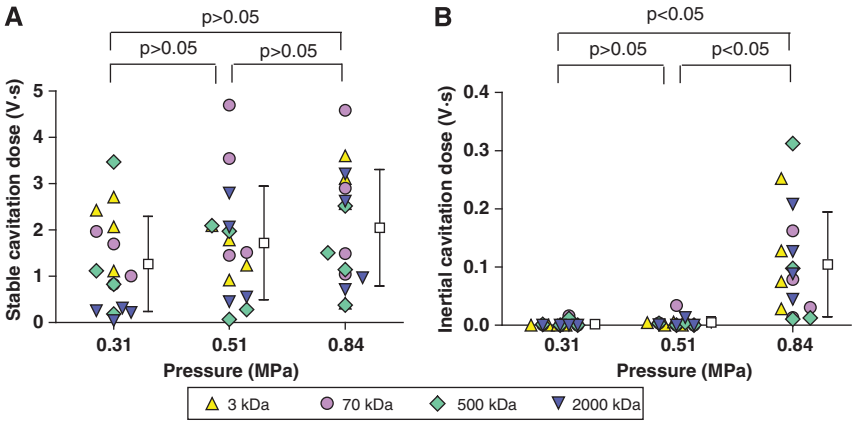

Figure 4. (**A**) Stable cavitation dose (SCD) and (**B**) inertial cavitation dose (ICD) at 0.31, 0.51, and 0.84 MPa for the four different-molecular weight dextrans. Different symbols represent dextrans with different MWs. The mean SCD shows a trend of increase with pressure; however, there were no significant difference with the pressure used. A significant increase ($P < 0.05$) in ICD was observed at 0.84 MPa only.

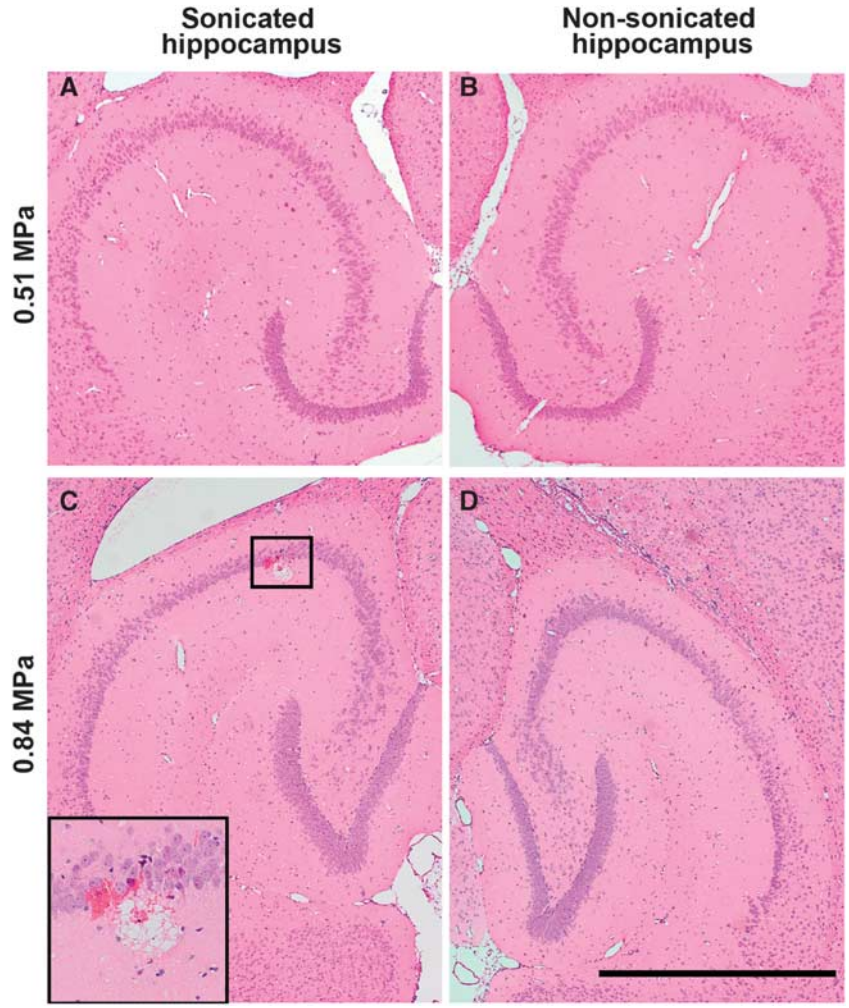

Figure 5. Microscopic examination of (**A**, **C**) left (sonicated) and (**B**, **D**) the corresponding right (nonsonicated) hippocampi in hemotoxylin and eosin stained, 6-μm-thick horizontal sections. No microscopic tissue damage was observed in the left hippocampus sonicated at 0.51 MPa (**A**), same as in the nonsonicated right hippocampus on the same section (**B**). Minor microhemorrhage was detected in one location (box) in the hippocampus sonicated at 0.84 MPa (**C**), compared with no damage in nonsonicated hippocampus (**D**). The insert shows a magnified image of the region in the box. Scale bar represents 1 mm.

Focused Ultrasound-Induced Blood–Brain Barrier Opening

Using fluorescent-labeled dextrans with different MWs, this study found that the BBB opening size depended on the acoustic pressure. The BBB opening size was smaller than 3 kDa ($D_H \sim 2.3$ nm) at 0.31 MPa, up to 70 kDa ($D_H \sim 10.2$ nm) at 0.51 MPa, and up to 2,000 kDa ($D_H \sim 54.4$ nm) at 0.84 MPa. This finding is

critical for developing FUS as a technology platform for the targeted trans-BBB delivery of agents with various sizes, as it revealed for the first time that FUS-induced BBB opening size is controllable by adjusting the acoustic parameters. Compared with all the neurosurgical, pharmacologic, or physiologic strategies that have been developed for delivering therapeutics to the brain,[1] FUS, as shown by the present study, is the only technique that can induce size-controllable BBB opening, allowing size-selective trans-BBB delivery.

These findings support the feasibility of designing therapeutic agent-size specific FUS treatment protocols. For instance, for the trans-BBB delivery of neurotrophins, such as brain-derived neurotrophic factor (MW $\sim$27 kDa, D_H $\sim$4.8 nm), an acoustic pressure of 0.51 MPa may be selected for initial testing with other parameters kept the same as the present study. However, for the efficient delivery of gene vectors, such as most recombinant adeno-associated virus vectors (MW $\sim$4 MDa, D_H $\sim$24 nm), the pressure may need to be increased to 0.84 MPa and sonication at multiple locations may be needed to enhance their spatial distribution in the hippocampus. We note that molecular size is a major determinant of passage across the BBB and used most commonly to define BBB permeability. However, BBB permeation also depends on a number of other physicochemical properties of the drugs, such as net overall charge and lipophilicity. Moreover, the affinity for carrier- or receptor-mediated transport, hydrogen bonding potential, and affinity for efflux mechanisms are further factors regulating the permeability of the BBB.[27] Therefore, other factors should be taken into consideration when extending the reported findings for dextrans to other agents.

The present study showed that the BBB opening size depended on the acoustic pressure, which is one of the most critical parameters determining MB cavitation behaviors. Other FUS parameters (for example, frequency, pulse length, and pulse-repetition frequency), as well as MB characteristics (for example, resonant frequency, size, and shell properties) may also be correlated with BBB opening size. For example, one previous study by our group found that the BBB opening pressure threshold for the delivery of 3 kDa dextran was significantly lower with MBs of 4 to 5 μm than 1 to 2 μm in diameter,[28] which suggests that MB size may be an important factor influencing the BBB opening size. The impact of parameters other than acoustic pressure on the BBB opening size will be the focus of future studies. In addition, future study will also explore the possibility to achieve finer control of the BBB opening size by adjusting acoustic pressures at a smaller incremental step and using dextrans of various MWs besides those tested in the current study.

This size selectivity of FUS-enhanced BBB permeability has implications in our understanding of the cellular mechanisms of FUS-induced BBB opening. Two main routes exist for the transport of molecules across the BBB: paracellular and transcellular pathways. Vesicular transport is size independent as vesicles are much larger than most therapeutic agents; however, transport *via* tight junction is size dependent: only molecules smaller than the gaps between tight junctions can go through.[9,10] Our results showed a size selectivity of molecular transport across the FUS-induced BBB opening, suggesting that paracellular transport through altered tight junctions may be the predominant cellular mechanism for FUS-induced BBB opening. Several potential cellular mechanisms for FUS-enhanced paracellular transport have been proposed, such as disassembling of tight junction proteins,[29] disruption of the interaction between tight junction proteins,[30] or reorganization of gap junction proteins.[31] The effect of FUS upon tight junctions has been reported to be transient and reversible.[29–31] Future studies are needed to elucidate how FUS and MBs interact at the molecular level of the BBB.

Microbubble Cavitation Emissions

Passive cavitation detection has been explored for remote real-time monitoring, feedback control, and outcome prediction of BBB opening.[17,18,20,22] However, it has been used only for cavitation detection during FUS-enhanced delivery of magnetic resonance imaging contrast agents (MW $<$ 1 kDa)[17,18,20,22] and 3 kDa dextran.[23] In this study, it was used for the first time to monitor the MB cavitation behaviors associated with the trans-BBB delivery of different-size agents. It was found that the cavitational mechanisms were different for the significant delivery of different-size agent, indicating that the PCD can be used to monitor MB activity and predict the BBB opening size.

For the relatively smaller-size dextrans (3 and 70 kDa) tested in this study, trans-BBB delivery by FUS-induced BBB opening was achieved with SC only. The IC threshold was found to be between 0.51 and 0.84 MPa. This threshold was higher than the pressure threshold (0.51 MPa) that led to the statistically significant increases in the delivery of 3 and 7 kDa dextrans, indicating that BBB opening can be achieved without IC for these two relative smaller molecules. This finding was consistent with previous PCD studies showing that agents with MW $\leqslant$ 3 kDa were successfully delivered across the BBB with SC only.[20–23] Our histologic evaluation showed that at 0.51 MPa no microscopic tissue damage was observed (Figure 5A), which was in good agreement with a growing body of literature showing that SC only can induce BBB opening without any evident tissue damage.[17–20]

For the relatively larger-size dextrans (500 and 2,000 kDa), IC was found to be the main mechanism for their successful trans-BBB delivery. Cavitation detection has not been reported in previous studies of FUS-enhanced delivery of larger agents, such as antibodies[4,32–34] and gene vectors,[5,35,36] whose MWs are on the same scale as the 500 and 2,000 kDa dextran, respectively. The MI of the FUS used in those studies varied within the range of 0.63 to 1.56, and the MI corresponding to 0.84 MPa (1.5 MHz) in our study was 0.69, which was in the lower end of the aforementioned range. This indicates that IC may be associated with the delivery of the reported antibodies and gene vectors, which was further supported by the observation of microhemorrhages and petechial hemorrhages in those studies that performed histologic analyses after FUS sonication.[5,33,35,36] The findings of our histologic analysis of mouse brains sonicated at 0.84 MPa (Figure 5C) were consistent with the minor microscopic damaging effects reported in those studies. Behavioral tests performed in nonhuman primates after repeated FUS sonication in combination with MBs showed that the procedure did not cause functional damage even in the presence of minimal histologic damage, such as tiny clusters of extravasated red blood cells and a few dark neurons.[20] It should be pointed out that full safety assessment is more complex than the preliminary histological analysis reported here and future work is needed to fully describe the safety profile of the FUS technique before its clinical translation. Nevertheless, it is clear that this technique causes less damage than the aforementioned invasive methods currently in the clinic for localized brain drug delivery, such as intracerebral-ventricular infusion, convection-enhanced delivery, or implantation of delivery systems.[37]

CONCLUSION

This study assessed the FUS-induced BBB opening size using molecules with different MWs and explored the physical mechanisms for the delivery of different-size agents. For the first time, we showed that FUS is so far the only technique that can induce size-controllable BBB opening, allowing size-selective trans-BBB delivery. The BBB opening size was smaller than 3 kDa (D_H $\sim$2.3 nm) at 0.31 MPa, increased up to 70 kDa (D_H $\sim$20.4 nm) at 0.51 MPa, and further increased up to 2,000 kDa (D_H $\sim$54.4 nm)

at 0.84 MPa. Meanwhile, the BBB opening size was found to be dictated by the cavitational mechanisms: a significant enhancement in the delivery of relative smaller-size agents (3 and 70 kDa) was achieved with SC only; however, IC was associated with the successful delivery of relative larger-size agents (500 and 2,000 kDa). Only minimal microscopic damage was noticeable in the sonicated region with IC, while no microscopic damage was observed with SC only. This study provided new insight into the fundamental mechanisms of FUS-induced BBB opening. More importantly, it is indicative of the potential for designing agent size-specific FUS treatment protocols and predicting the BBB opening size using PCD.

DISCLOSURE/CONFLICT OF INTEREST

The authors declare no conflict of interest.

ACKNOWLEDGMENTS

The authors would like to thank Camilo Acosta, Anushree Srivastava, Oluyemi Olumolade, Tao Sun, Cherry C Chen, Shutao Wang and Gesthimani Samiotaki from the Department of Biomedical Engineering, Columbia University, for their assistant and suggestions.

REFERENCES

1 Pardridge WM. Drug transport across the blood-brain barrier. *J Cereb blood flow Metab* 2012; **32**: 1959–1972.
2 Treat LH, McDannold N, Zhang Y, Vykhodtseva N, Hynynen K. Improved anti-tumor effect of liposomal doxorubicin after targeted blood-brain barrier disruption by MRI-guided focused ultrasound in rat glioma. *Ultrasound Med Biol* 2012; **38**: 1716–1725.
3 Baseri B, Choi JJ, Deffieux T, Samiotaki G, Tung Y-S, Olumolade O *et al.* Activation of signaling pathways following localized delivery of systemically administered neurotrophic factors across the blood-brain barrier using focused ultrasound and microbubbles. *Phys Med Biol* 2012; **57**: N65–N81.
4 Jordão JF, Thévenot E, Markham-Coultes K, Scarcelli T, Weng Y-Q, Xhima K *et al.* Amyloid-ß plaque reduction, endogenous antibody delivery and glial activation by brain-targeted, transcranial focused ultrasound. *Exp Neurol* 2013; **248**: 16–29.
5 Huang Q, Deng J, Wang F, Chen S, Liu Y, Wang Z *et al.* Targeted gene delivery to the mouse brain by MRI-guided focused ultrasound-induced blood-brain barrier disruption. *Exp Neurol* 2012; **233**: 350–356.
6 Konofagou EE, Tung Y-S, Choi J, Deffieuxa T, Baseria B, Vlachosa F. Ultrasound-induced blood-brain barrier opening. *Curr Pharm Biotechnol* 2012; **13**: 1332–1345.
7 Burgess A, Hynynen K. Noninvasive and targeted drug delivery to the brain using focused ultrasound. *ACS Chem Neurosci* 2013; **8588**: 1–7.
8 Sheikov N, McDannold N, Vykhodtseva N, Jolesz F, Hynynen K. Cellular mechanisms of the blood-brain barrier opening induced by ultrasound in presence of microbubbles. *Ultrasound Med Biol* 2004; **30**: 979–989.
9 Heistad D. Permeability of blood-brain barrier to various sized molecules. *Am J Physiol Circ Physiol* 1985; **248**: H712–H718.
10 Robinson PJ, Rapoport SI. Size selectivity of blood-brain barrier permeability at various times after osmotic opening Size selectivity of blood-brain barrier permeability various times after osmotic opening. *Am J Physiol Regul Integr Comp Physiol* 1987; **253**: R459–R466.
11 Choi JJ, Wang S-G, Tung Y-S, Morrison B, Konofagou EE. Molecules of various pharmacologically-relevant sizes can cross the ultrasound-induced blood-brain barrier opening in vivo. *Ultrasound Med Biol* 2010; **36**: 58–67.
12 Marty B, Larrat B, Van Landeghem M, Robic C, Robert P, Port M *et al.* Dynamic study of blood-brain barrier closure after its disruption using ultrasound: a quantitative analysis. *J Cereb Blood Flow Metab* 2012; **32**: 1948–1958.
13 Deng CX. Targeted drug delivery across the blood-brain barrier using ultrasound technique. *Ther Deliv* 2010; **1**: 819–848.
14 Van Wamel A, Kooiman K, Harteveld M, Emmer M, ten Cate FJ, Versluis M *et al.* Vibrating microbubbles poking individual cells: drug transfer into cells via sonoporation. *J Control Release* 2006; **112**: 149–155.
15 Tung Y-S, Vlachos F, Feshitan JA, Borden MA, Konofagou EE. The mechanism of interaction between focused ultrasound and microbubbles in blood-brain barrier opening in mice. *J Acoust Soc Am* 2011; **130**: 3059–3067.
16 Chen H, Kreider W, Brayman AA, Bailey MR, Matula TJ. Blood vessel deformations on microsecond time scales by ultrasonic cavitation. *Phys Rev Lett* 2011; **106**: 034301.
17 McDannold N, Vykhodtseva N, Hynynen K. Targeted disruption of the blood-brain barrier with focused ultrasound: association with inertial cavitation. *Phys Med Biol* 2006; **2**: 793–807.
18 Tung Y-S, Vlachos F, Choi JJ, Deffieux T, Selert K, Konofagou EE. In vivo transcranial cavitation detection during ultrasound-induced blood-brain barrier opening. *Phys Med Biol* 2010; **55**: 6141–6155.
19 Baseri B, Choi JJ, Tung Y-S, Konofagou EE. Multi-modality safety assessment of blood-brain barrier opening using focused ultrasound and definity microbubbles: a short-term study. *Ultrasound Med Biol* 2010; **36**: 1445–1459.
20 McDannold N, Arvanitis CD, Vykhodtseva N, Livingstone MS. Temporary disruption of the blood-brain barrier by use of ultrasound and microbubbles: safety and efficacy evaluation in rhesus macaques. *Cancer Res* 2012; **72**: 3652–3663.
21 McDannold N, Vykhodtseva N, Raymond S, Jolesz FA, Hynynen K. MRI-guided targeted blood-brain barrier disruption with focused ultrasound: histological findings in rabbits. *Ultrasound Med Biol* 2005; **31**: 1527–1537.
22 O'Reilly MA, Hynynen K. Feedback-controlled focused ultrasound disruption by using an acoustic emissions-based controller. *Radiology* 2012; **263**: 96–106.
23 Chen CC, Sheeran PS, Wu S-Y, Olumolade OO, Dayton Pa, Konofagou EE. Targeted drug delivery with focused ultrasound-induced blood-brain barrier opening using acoustically-activated nanodroplets. *J Control Release* 2013; **172**: 795–804.
24 Choi JJ, Pernot M, Small SA, Konofagou EE. Noninvasive, transcranial and localized opening of the blood-brain barrier using focused ultrasound in mice. *Ultrasound Med Biol* 2007; **33**: 95–104.
25 Lebrun L, Junter G-A. Diffusion of dextran through microporous membrane filters. *J Memb Sci* 1994; **88**: 253–261.
26 Tung Y-S, Marquet F, Teichert T, Ferrera V, Konofagou EE. Feasibility of non-invasive cavitation-guided blood-brain barrier opening using focused ultrasound and microbubbles in nonhuman primates. *Appl Phys Lett* 2011; **98**: 163704.
27 Tamai I, Tsuji A. Drug delivery through the blood-brain barrier. *Adv Drug Deliv Rev* 1996; **19**: 401–424.
28 Choi JJ, Feshitan JA, Baseri B, Wang S, Tung Y-S, Borden MA *et al.* Microbubble-size dependence of focused ultrasound-induced blood-brain barrier opening in mice in vivo. *IEEE Trans Biomed Eng* 2010; **57**: 145–154.
29 Sheikov N, McDannold N, Sharma S, Hynynen K. Effect of focused ultrasound applied with an ultrasound contrast agent on the tight junctional integrity of the brain microvascular endothelium. *Ultrasound Med Biol* 2008; **34**: 1093–1104.
30 Jalali S, Huang Y, Dumont DJ, Hynynen K. Focused ultrasound-mediated BBB disruption is associated with an increase in activation of AKT: experimental study in rats. *BMC Neurol* 2010; **10**: 114.
31 Alonso A, Reinz E, Jenne JW, Fatar M, Schmidt-Glenewinkel H, Hennerici MG *et al.* Reorganization of gap junctions after focused ultrasound blood-brain barrier opening in the rat brain. *J Cereb Blood Flow Metab* 2010; **30**: 1394–1402.
32 Kinoshita M, McDannold N, Jolesz FA, Hynynen K. Noninvasive localized delivery of Herceptin to the mouse brain by MRI-guided focused ultrasound-induced blood–brain barrier disruption. *Proc Natl Acad Sci USA* 2006; **103**: 11719–11723.
33 Jordão JF, Ayala-Grosso CA, Markham K, Huang Y, Chopra R, McLaurin J *et al.* Antibodies targeted to the brain with image-guided focused ultrasound reduces amyloid-beta plaque load in the TgCRND8 mouse model of Alzheimer's disease. *PLoS ONE* 2010; **5**: e10549.
34 Raymond SB, Treat LH, Dewey JD, McDannold NJ, Hynynen K, Bacskai BJ. Ultrasound enhanced delivery of molecular imaging and therapeutic agents in Alzheimer's disease mouse models. *PLoS ONE* 2008; **3**: e2175.
35 Alonso A, Reinz E, Leuchs B, Kleinschmidt J, Fatar M, Geers B *et al.* Focal delivery of AAV2/1-transgenes into the rat brain by localized ultrasound-induced BBB opening. *Mol Ther Nucleic Acids* 2013; **2**: e73.
36 Hsu P-H, Wei K-C, Huang C-Y, Wen C-J, Yen T-C, Liu C-L *et al.* Noninvasive and targeted gene delivery into the brain using microbubble-facilitated focused ultrasound. *PLoS ONE* 2013; **8**: e57682.
37 Gabathuler R. Approaches to transport therapeutic drugs across the blood-brain barrier to treat brain diseases. *Neurobiol Dis* 2010; **37**: 48–57.